Electrical Power and Energy Systems 44 (2013) 461–470

Contents lists available at SciVerse ScienceDirect

Electrical Power and Energy Systems

journal homepage: www.elsevier.com/locate/ijepes

Optimal IPFC signal selection and damping controller design using a novel current injection model in a multi-machine power system

Navid Rezaei *, Mohsen Kalantar, Heidar Ali Shayanfar, Yosef Alipouri, Amin Safari

Center of Excellence for Power System Automation and Operation, Department of Electrical Engineering, Iran University of Science and Technology, Narmak 16846 13114, Tehran, Iran

ARTICLE INFO

Article history:
Received 3 February 2012
Received in revised form 20 June 2012
Accepted 31 July 2012
Available online 26 September 2012

Keywords:
Power system stability enhancement
IPFC
Current injection model
Particle Swarm Optimization

ABSTRACT

This paper develops a novel approach to model the Interline Power Flow Controller (IPFC) with the purpose of enhancing the power system dynamic stability. The dynamic behavior of the IPFC is modeled using a new and detailed current injection model. On the basis of designing a supplementary damping controller, the effectiveness of the proposed model in robust damping of the oscillations is evaluated. Thus, the problem of attaining the damping controller parameters transmitted into an optimization process which is solved using Particle Swarm Optimization algorithm (PSO). The PSO has a strong and reliable capability to find out the optimistic solution. The optimization procedure is performed in a multi-machine power system and under various operating conditions. Assessment the derived results from the nonlinear time domain simulation and through some performance indices with considering to a severe transient disturbance clearly indicates the major performance of the proposed model and the model based designed controller in improvement the system stability margins. Moreover, to identify the most suitable IPFC control signal, a precise evaluation of the employed indices is accomplished. Numerical results verify the superior stabilization effect of the m_1 (one of the IPFC control signals) in the wide range of operating conditions.

1. Introduction

Nowadays, due to the deregulation of electricity market and increasing in the power demand, power systems operate close to their stability limits. On the other hand, the inevitable electromechanical oscillations can cause the restriction of power transfer capability and thus threaten the secure and stable operation of the power system. In such under-stressed system, reinforcement the system flexibility and stability characteristics is an enterprise which lionized by many researches. So, it seems to be necessary to utilize some stabilizers to provide the loadable, robust and stable operating margins to the power system [1,2]. Conventionally, Power System Stabilizers (PSSs) are used to confirm these requirements. However, with reference to the inherent problems of the PSSs, especially inadequate mitigation of the inter-area oscillatory modes in the case of the long transmission lines, and regarding to the ever-increasing progress in the field of power electronics technology, it seems that Flexible AC Transmission System (FACTS) devices are more beneficial alternative for the purpose of power system static and dynamic performance improvement [3]. Recently, Interline Power Flow Controller (IPFC) has been emerged as one of the versatile initiatives of FACTS family [4]. In the IPFC, two or more Voltage Source Converters (VSCs) are linked together through a common DC capacitor to simultaneously and separately control more than one transmission lines. In this scheme, by exchanging the active and reactive power flow between the compensated lines, IPFC can develop a robust control of power flow in the transmission network, thus in light of the optimal techno-economical operation, it is necessary to investigate the IPFC's ability in enhancement the stability and damping issues of the power systems. In recent years, some of the researchers [5–7] investigate the application of the IPFC for power oscillation damping. In [5], Mishra et al. by proposing a power injection based model to the IPFC addressed an efficient hybrid optimization framework in the terms of the combination of GA and neural-fuzzy algorithms to investigate the power system transient stability improvement. However, their study did not include any effort to determine the suitable control signals of the IPFC. There are different modeling of the IPFC corresponding to the application purpose and the case study power systems. Substantially, in the stability studies the validity of the results is greatly dependent to the accuracy of the system modeling. According to the administrative role of the FACTS devices in the terms of power oscillation damping, different models such as linearized Heffron–Phillips [7,8], power injection [5,15], energy function [9] and voltage source based model [10] can be found in the literature. Some of the aforementioned modeling methodologies, e.g. the power injection based models, are

* Corresponding author. Tel.: +98 9188772448; fax: +98 77322562.
E-mail address: nrezaei@iust.ac.ir (N. Rezaei).

0142-0615/$ - see front matter © 2012 Elsevier Ltd. All rights reserved.
http://dx.doi.org/10.1016/j.ijepes.2012.07.071

substantially derived with the purpose of utilization in the steady-state studies. Besides, in the others that they are more adaptable to dynamic or transient investigations some are useful for the linear-modeled and particularly for the small size case studies such as Heffron–Phillips and some others are suitable for nonlinear and high dimension systems like energy function based or current injection models. Hereinafter, as regards to the adoption of current balance equations in many dynamic simulation programs, a novel current injection model for the IPFC is taken into account. The primary reason for this approach is the high compatibility and universality of the current injection models to the traditional procedure of the power system analysis. For example, the voltage source based models change the admittance matrix of power system while in the system analyzing processes the admittance matrix should be constant and symmetrical. However, in the proposed current injection model, it is trying to replace the series injected voltage by shunt current sources which are described using nonlinear equations. Thus turning to the similar behavior of the shunt sources to the nature of the loads, the system admittance matrix is not changed significantly through this modeling [11]. The proposed model is not only suitable for stability purposes, but it also gives faster and a wider area of convergence in the power flow analysis [12]. Nonlinear equations describing the precise dynamic behavior of the IPFC are another advantage of this model. The drawback of linear approaches is that they may lead to inadequate damping, in the case of disturbances, especially in large realistic power systems where more dynamic equipments are interconnected and then enhance the coupling effect and order of the system [24]. Generally, despite the efficiency and reliability of linear models in the single machine power systems, they may face to inefficiency and incompetence in larger systems. Although, in recent years, some researches utilize current injection model to the different FACTS devices such as TCSC[1] [13], SSSC[2] [14] and UPFC[3] [12], however, to the best of our knowledge most of the researches are focuses on the simplification the Optimal Power Flow (OPF) problem [15–19] and dare could be said that no work has been developed on the extraction of current based model for the dynamic performance evaluation of the IPFC. In short, the main contribution of this paper is to bring out a universal and less problematic current injection model for the IPFC and evaluate its dynamic performance in a multi-machine power system. The power system is employed by this study, is the IEEE standard 4-machine two area test system. It is considered to be operated with all the essential and itemized stability required dynamics. Though, it is not as comprehensive as a large scale realistic power system, by thorough investigation of the dynamic aspects of the system and considering the local measuring signals, the basic characteristics and detailed interactive performance of the system controllers can be well estimated and the extracted conclusions through an insight perspective may be eligible to effectively generalize for implementation in the high dimensional test power systems [26].

On the other hand, due to the nonlinear nature and existing uncertainties of the power system, FACTS devices may not able to produce sufficient damping torque to oscillatory modes, therefore, prediction and deployment a supplementary FACTS-based controller with high flexibility and adaptable parameters to the power system different operating conditions seem to be necessary [7]. The great challenge in the controller design procedure is to choose an appropriate design strategy. In this study, according to the more industrial aspect of lead-lag controller scheme, it is employed to be utilized as the damping controller. With the knowledge of the multimodal nature (more than one local optima) of this controller, it should be employed a robust optimization method to find the global optimal parameters. Application of fuzzy logic, neural networks and robust control methodologies as reported in some literatures may be efficient in some cases [5,6]. However, adjustment the initial conditions of these algorithms needs more warranty and is usually on the basis of trial and error. Also in some cases, they are infeasible to be implemented to the power system dynamic equations [13]. In the last decades, the meta-heuristic algorithms are applied to several engineering problems as useful optimization tools. One of these algorithms is Particle Swarm Optimization (PSO) which is a dynamic explorer to entice the global or near-global optimum. It has a great perceptivity to accommodate to the nature of the objective functions and is able to produce the acceptable quality of solutions with minimum fitness evaluations [20,21]. Moreover, with the aim of achieving a tech-economical operation and reach to the desired secure stability margins, selection an appropriate control signal among the FACTS different signals is vital. In the case of the IPFC as a versatile compensator the problem is more crucial. Thus, the paper directs to find out the optimistic control signal of the IPFC through the proposed PSO-based optimization framework. In the proposed framework, the performance of the PSO algorithm is compared to two heuristic algorithms, i.e. Genetic Algorithm and Classic Evolutionary Programming to ensure that the global or near global optimal solution is achieved.

In this paper, the PSO algorithm is employed to find the optimal set of the IPFC damping controller parameters. The objective function is formulated into the way that ensures the robustness of the dynamic response of the power system to some severe disturbances and under various operating conditions. The performance of the proposed current injection model of the IPFC is investigated in a two-area four machine power system under various operating conditions. Moreover, the efficiency of the four control signals of the IPFC (m_1, δ_1, m_2 and δ_2) is assessed through the time-domain simulation and some performance indices evaluations. Analyzing the results represents the parturiency of the PSO based designed controllers, corresponding to each control signal, and verify the predominance of the novel current injection model in good damping the power oscillations and enhancement the overall system stability. Furthermore, in order to optimize the IPFC operational costs and intensify the stabilizer signal, the optimal control signal of the IPFC is assessed and consequently, the m_1 based damping approach shows more potential to robust control of the oscillatory modes. Besides, the results of the PSO algorithm are evaluated by comparison to the GA and CEP algorithms.

2. Current Injection model of the IPFC

IPFC is one the VSC based FACTS devices which provides a benefactress management of power flow in the parallel or multiline corridors and is able to improve the dynamic and transient stability of the power system. For an IPFC with two VSCs, there are four control signals in the terms of m_1, δ_1, m_2 and δ_2 which are the magnitude and angle of the series injected voltages of the VSC 1 and 2, respectively. The voltage profile and active and reactive power flows could be set out by managing the control signals. The configuration of the IPFC with two series branches is shown in Fig. 1. In this scheme, the IPFC proper function is required that the total active powers injected into or absorbed from the lines be zero, which refers to that in the IPFC structure, one of the VSCs (master) can freely exchange active power flow with the underutilized lines, and coordinately the other (slave) has to be regulated in order to satisfy the Eq. (1) [4]:

$$P_{se1} + P_{se2} = 0 \tag{1}$$

[1] Thyristor Controlled Series Capacitor.
[2] Static Synchronous Series Compensator.
[3] Unified Power Flow Controller.

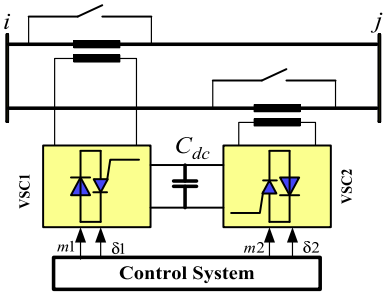

Fig. 1. The configuration of IPFC with two VSCs.

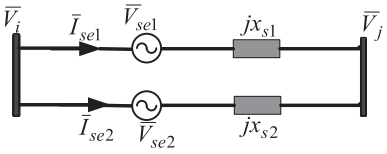

Fig. 2. The equivalent voltage source based IPFC model.

P_{se1} and P_{se2} are the injected active power of the VSC1 and VSC2, respectively.

The assumed IPFC in Fig. 1 can be modeled with two series voltage sources as represented in Fig. 2. The voltages of the buses and VSCs have the following equations:

$$\overline{V}_i = V_i e^{j\theta_i},\ \overline{V}_j = V_j e^{j\theta_j} \tag{2}$$

$$\overline{V}_{se1} = m_1 \overline{V}_i e^{j\delta_1} \tag{3}$$

$$\overline{V}_{se2} = m_2 \overline{V}_i e^{j\delta_2} \tag{4}$$

By substitution the voltage sources with their equivalent current sources, and assuming that the master VSC is the VSC2, the injected current of the slave VSC (VSC1) has to establish the active power equality equation (Eq. (1)) constraint. Thus, considering to Fig. 3, the VSCs current injection equations are described as following:

$$\overline{I}_{inj2} = \frac{\overline{V}_{se2}}{jx_{s2}} = -jb_{s2}\overline{V}_{se2} \tag{5}$$

$$\overline{I}_{inj2} = m_2 b_{s2} V_i e^{j(\theta_i+\delta_2-\pi/2)} \tag{6}$$

where b_{S2} is the imaginary part of the admittance corresponding to the line 2. The real and imaginary parts of the apparent power of the VSC2 are calculated using Fig. 2.

$$S_{se2} = [\overline{V}_{se2} \cdot \overline{I}^*_{se2}] = \left[m_2 V_i e^{j(\theta_i+\delta_2)} \cdot \left(\frac{\overline{V}_i - \overline{V}_j + m_2 V_i e^{j(\theta_i+\delta_2)}}{jx_{s2}} \right)^* \right] \tag{7}$$

$$P_{se2} = \mathrm{Re}[S_{se2}] = m_2 b_{s2}[V_i V_j \sin(\theta_i - \theta_j + \delta_2) - V_i^2 \sin\delta_2] \tag{8}$$

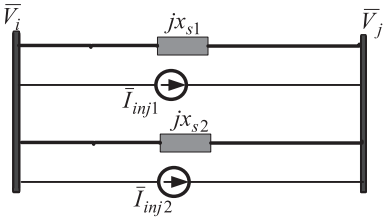

Fig. 3. Substitution the series voltage source by the current injection sources.

$$Q_{se2} = \mathrm{Imag}[S_{se2}] = m_2 b_{s2}\left[V_i V_j \cos(\theta_i - \theta_j + \delta_2) - V_i^2 \cos\delta_2 - m_2^2 V_i^2\right] \tag{9}$$

It is assumed that the VSC1 injects a current with the Eq. (10).

$$\overline{I}_{inj1} = I_{inj1} e^{j\beta} \tag{10}$$

To satisfy the equality constraint described in Eq. (1), from Fig. 3, the apparent power of the VSC1 is calculated as follows:

$$S_{se1} = [\overline{V}_{se1} \cdot \overline{I}^*_{se1}] = \left[\frac{\overline{I}_{inj1}}{-jb_{s1}} \cdot I^*_{se1} \right] \tag{11}$$

$$S_{se1} = [-I_{inj1} e^{j\beta} \cdot (V_i e^{-j\theta_i} - V_j e^{j\theta_j} + m_1 V_i e^{-j(\theta_i+\delta_1)})] \tag{12}$$

$$\begin{aligned} P_{se1} &= \mathrm{Re}[S_{se1}] \\ &= -I_{inj1} \cdot [V_i \cos(\beta - \theta_i) - V_j \cos(\beta - \theta_j) + m_1 V_i \cos(\beta - \theta_i - \delta_1)] \end{aligned} \tag{13}$$

$$\begin{aligned} Q_{se1} &= \mathrm{Im}ag[S_{se1}] \\ &= -I_{inj1} \cdot [V_i \sin(\beta - \theta_i) - V_j \sin(\beta - \theta_j) + m_1 V_i \sin(\beta - \theta_i - \delta_1)] \end{aligned} \tag{14}$$

According to the Eq. (1), the I_{inj1} could be written as:

$$I_{inj1} = \frac{m_2 b_{s2}[V_i V_j \sin(\theta_i - \theta_j + \delta_2) - V_i^2 \sin\delta_2]}{V_i \cos(\beta - \theta_i) - V_j \cos(\beta - \theta_j) + m_1 V_i \cos(\beta - \theta_i - \delta_1)} \tag{15}$$

As the result, the proposed current injection model of the IPFC can be shown by two equivalent shunt current source which are installed in the buses as represented in Fig. 4. The current sources are demonstrated using the Eqs. (16) and (17). The x_S is the equivalent reactance of the two parallel branches. The line resistance and the reactances of the boosting transformers are neglected.

$$\overline{I}_{si} = \overline{I}_{inj1} + \overline{I}_{inj2} \tag{16}$$

$$\overline{I}_{si} = -\overline{I}_{sj} \tag{17}$$

The proposed current injection model not only describes the detailed dynamic behavior of the IPFC but it also helps decreasing the computational calculations by not changing the system admittance matrix. This is because of that the current injected models substitute in the system current matrix.

The derived current injection model of the IPFC is applied to the four machine and two area power system as shown in Fig. 5. In the nominal operation, there is a power transfer flow within 413 MW from area 1 to area 2. The IPFC is assumed to be installed through the current injection model between buses 8 and 9. Note that the power system performance analysis is performed under the nonlinear equations of the generators. The considered nonlinear equations of the ith generator are [1,25]:

$$\dot{\delta}_i = \omega_0(\omega_i - 1) \tag{18}$$

$$\dot{\omega}_i = \frac{P_{mi} - P_{ei} - D_i(\omega_i - 1)}{M_i} \tag{19}$$

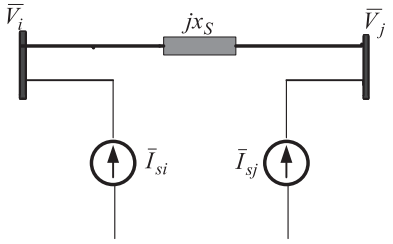

Fig. 4. The proposed IPFC current injection model.

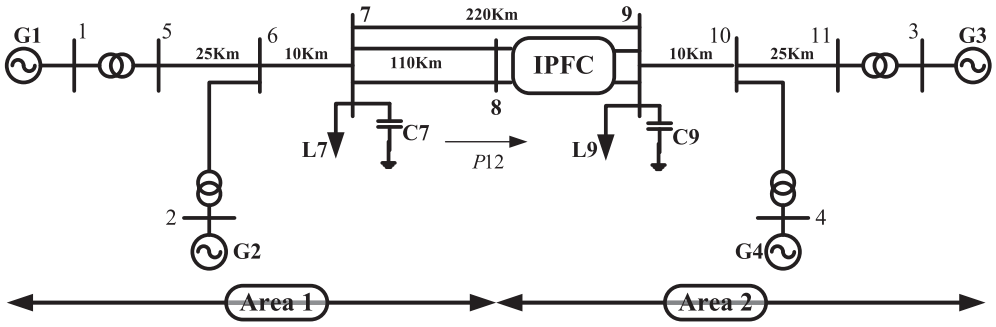

Fig. 5. The four machine two area test power system.

$$\dot{E}'_{qi} = \frac{E_{fdi} - (x_{di} - x'_{di})i_{di} - E'_{qi}}{T'_{doi}} \tag{20}$$

$$\dot{E}_{fdi} = \frac{K_{Ai}(V_{refi} - V_{ti}) - E_{fdi}}{T_{Ai}} \tag{21}$$

$$T_{ei} = E'_{qi}i_{qi} - (x_{di} - x'_{di})i_{di}i_{qi} \tag{22}$$

Where, δ, ω, P_m, P_e, E'_q, E_{fd}, T_e, T'_{do}, K_A, T_A, V_{ref} and V_t denote rotor angle, rotor speed, mechanical input power, electrical output power, internal voltage behind x'_d, equivalent excitation voltage, electric torque, time constant of excitation circuit, AVR gain, AVR time constant, reference voltage and terminal voltage, respectively.

In the considered test power system, in order to better simulation, the loads are assumed to treat as constant impedance loads. The PSSs' control signals in both areas are neglected in this study. The detailed power system data are given in [25].

3. Optimization framework

In order to find out the optimum solution of the problem of the IPFC control signal selection and supplementary damping controller design, an optimization framework is proposed to give an assurance to the optimization problem in the viewpoint of attaining the global optimal or at least a near global optimal solution. The proposed optimization framework includes three prevalent heuristic optimizers, i.e. Particle Swarm Optimization (PSO), Genetic Algorithm (GA) and Classic Evolutionary Programming (CEP) which are individually applied to the problem to discover the optimal solution. Then on the basis of some statistical evaluations the performance of the algorithms are assessed and compared to ensure finding the global optimal solution. In the following, whilst briefly introducing the fundamentals of the algorithms, the principles of the statistical approach are mentioned.

3.1. Particle Swarm Optimization

In the recent years, one of the most important stochastic global search algorithms and parallel evolutionary computation techniques which mimics the fauna social behavior, is Particle Swarm Optimization (PSO) algorithm. In 1995, the PSO algorithm is first proposed by Kennedy and Eberhart [22]. After that, PSO is increasingly applicant, like in medical treatment of human tremors in diseases such as Parkinson's disease [23]. The advantages of PSO, compared to other methods, are easily coding, computationally inexpensive in terms of both memory requirements and speed criteria [20], derivative-free suitable to continuous variable problems, adaptable convergence with the potential to yield better quality of solutions, except to the pre-mature convergence in complicated multi-peak search problem [21], adjustable to nonlinear combinational optimization problems from vast to limited solution space and insensitivity to convex, concave or discontinuous nature of the objective function. PSO uses the real-number randomness and the global communication among the swarm members called 'particle's. Because of the both stochastic and deterministic components of particle movements, each particle is attracted toward the position of the current global best while simultaneously it has tendency to move randomly [20–23]. As a result, an experience exchange occurs among the swarm particles and after each iteration the movement of each particle naturally evolves to an optimal solution. The PSO is initialized with a group of random particles and searches for the optimal point by updating generations. In each iteration, particles are updated by the best values of itself and the group's. The ith particle is represented by $X_i = (x_{i1}, x_{i2}, \ldots, x_{iD})$. Each particle keeps track of its coordinates in hyperspace, which are associated with the fittest solution it has achieved so far. The value of the fitness for particle i (*pbest*) is also stored as $P_i = (p_{i1}, p_{i2}, \ldots, p_{iD})$. The global version of the PSO keeps track of the overall best value (*gbest*), and its location, obtained thus far by any particle in the population. The PSO consists of, at each step, changing the velocity of each particle toward its *pbest* and *gbest* according to Eq. (23). The velocity of particle i is represented as $V_i = (v_{i1}, v_{i2}, \ldots, v_{iD})$. The position of the ith particle is then updated according to Eq. (24) [20].

$$v_{id}(t+1) = \omega v_{id}(t) + c_1 rand_1(P_{id}(t) - x_{id}(t)) + c_2 rand_2(P_{gd}(t) - x_{id}(t)) \tag{23}$$

$$\vec{x}(t+1) = \vec{x}(t) + \vec{v}(t+1) \tag{24}$$

where P_{id} and P_{gd} are *pbest* and *gbest*. In the PSO, the tradeoff between the local and global exploration abilities is mainly controlled by inertia weights (ω). The inertia weight which is formulated as in Eq. (25) decreases linearly from 0.9 to 0.4 during the run [20,21].

$$\omega = \omega_{max} - \left[\frac{\omega_{max} - \omega_{min}}{iter_{max}}\right] \cdot iter \tag{25}$$

where ω_{max} is the initial value of the inertia weight, ω_{min} is the final value of the inertia weight, $iter_{max}$ is the maximum iteration number and *iter* is the current iteration number. Fig. 6 shows the flowchart of the PSO algorithm.

3.2. Genetic Algorithm

A Genetic Algorithm is a mathematical search technique on the principles of natural selection and genetic recombination [28] which was firstly developed by John Holland. As one of its applications, it can be used as an optimization technique to find the minimum and maximum of the functions. In this case, a simple GA starts by randomly generating a population of chromosomes as possible solutions. The generated population is called a generation. The chromosomes of the current generation are evaluated for their fitness. The chromosomes with higher fitness scores are selected,

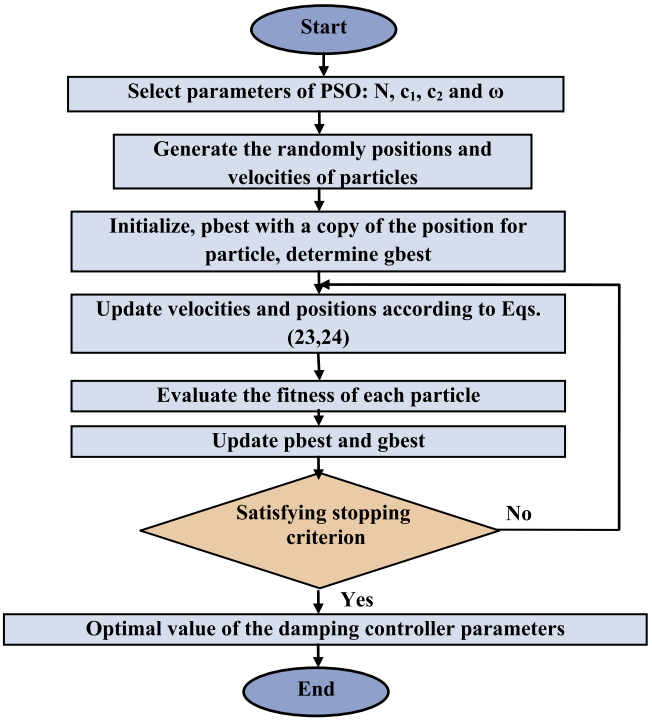

Fig. 6. The Particle Swarm Optimization algorithm flowchart.

with replacement, to create a mating pool. Then genetic operators of crossover and mutation are applied at this stage in a probabilistic manner. Crossover is used to produce new offspring from some selected chromosomes. Mutation can introduce traits not in the original population and keeps the GA from converging too fast before sampling the entire cost surface. At this stage, a new generation is produced and this procedure continues until a suitable termination condition is satisfied [29].

3.3. Classic Evolutionary Programming

The general format of Classic Evolutionary Programming (CEP) follows a two-step process of selection and variation in a population. Following initialization of a population, the fitness of each individual in the population is scored with respect to the cost function. In general, selection is applied as a tournament wherein the fitness of each individual in the population is compared against the fitness of a random set of other individuals in the same population. A "win" is recorded for an individual each time that individual's fitness equals or exceeds that of another in the tournament set. Individuals are then ranked with respect to the number of wins and those with the highest number of wins over some threshold are selected as parents for the next generation. Parents are randomly varied to generate offspring and the fitness of each member in the population is re-evaluated. This process is repeated for a user-specified number of generations [30].

3.4. Statistical test

In recent years, the use of statistical tests to improve the evaluation process of the performance of a new method has become a widespread technique in computational intelligence. Usually, they are employed inside the framework of any experimental analysis to decide when one algorithm is considered better than another.

This task, which may not be trivial, has become necessary to confirm whether a new proposed method offers a significant improvement, or not, over the existing methods for a given problem.

One of the most frequent situations where the use of statistical procedures is requested is in the joint analysis of the results achieved by various algorithms. The groups of differences between these methods usually associated with the problems met in the experimental study.

In this section, it is assigned a procedure to estimate the differences between several algorithms: the Contrast Estimation of medians. This method is very recommendable if it is assumed that the global performance is reflected by the magnitudes of the differences among the performances of the algorithms [31–33]. This methodology can be understood as an advanced global performance measure. It is especially useful to estimate by how far an algorithm outperforms another one [31].

4. Simulation results

In order to improve the damping of the power system oscillations, the function of the proposed damping controller is regulated in a way which generates an in-phase torque with the input signal. The damping controller output torque sustains the damping torque of the IPFC. The structure of the damping controller is opted as a conventional lead-lag structure. The simplicity, adaptability and industrial preference are the dominant reasons for this choice. In the damping controller as shown in Fig. 7., the input signal is the deviation of the tie-line power transfer signal from area 1 to area 2 ($\Delta P12$) and all four control signals of the IPFC (m_1, δ_1, m_2 and δ_2) are modulated. The tie line signal encompasses more dynamic data corresponding to the existing operational point.

The PSO algorithm is employed as the main algorithm to optimize the damping controller parameters (i.e., K, T_1, T_2, T_3 and T_4) as respect to minimize the following objective function [13]:

$$J = \int_0^{t_{sim}} t \cdot (|\omega_1 - \omega_2| + |\omega_1 - \omega_3| + |\omega_1 - \omega_4| + |\omega_3 - \omega_4|)dt$$
$$F = \sum_{i=1}^{N_P} J_i \quad (26)$$

where N_P is the number of the operating points which are listed in Table 1. These operating points are load flow results in the power system demonstrated in Fig. 5. ω_i is the speed of the ith generator and is derived by integration from the Eq. (19) and then the

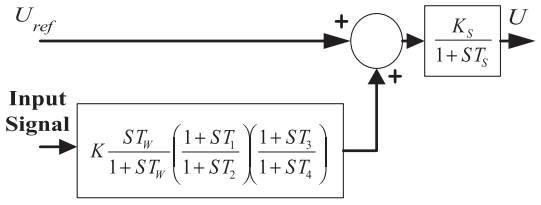

Fig. 7. The damping controller structure.

Table 1
The considered power system operating points.

Operating point	P_1	Q_1	P_2	Q_2	P_3	Q_3	P_4	Q_4
Case 1	0.7621	0.0835	0.7176	0.0671	0.8226	0.1331	0.7927	0.1362
Case 2	1.1511	0.1539	0.4622	0.0334	0.7667	0.0756	0.7667	0.0698
Case 3	0.5050	0.0519	0.9067	0.1155	0.8889	0.1163	0.8778	0.1065

difference between the speeds of the generators is measured in the SIMULINK environment. t_{sim} indicates the time duration in which the nonlinear time-domain simulation is ran.

The objective function is defined in due from to include both the inter area (zonal interactions) and the local (sympatric machine oscillations) modes of the oscillations. It is noteworthy that the inter-area modes are more significant in multi machine power systems. As it is denoted in the objective function, it is a the sum of the Integral of Time multiplied Absolute value of the Error (ITAE) performance indices corresponding to each operating point. The mainspring to choose the ITAE as the cornerstone of the objective function is that the ITAE performance index adds the simulation time (t) as a weighting factor to the deviation minimization process in order to contribute not only the magnitude of the standard deviation of the controller error known as a large error at the start of the disturbance, but it also considers small errors existing a long time after the disturbance and thus it guaranties the deviation minimization during the interval the controller is compensating. On the other hand, in the ITAE for the sake of using the absolute value of the error and restraining the error not to exceed than 1, it has more acceptability to its rival i.e. ITSE and is generally used.

Table 2
The optimized damping controller parameters using the PSO.

IPFC control signal	m_1	m_2	δ_1	δ_2
K	48.2101	61.0332	12.4490	6.6222
T_1	1.4021	1.0155	1.9011	0.9921
T_2	0.0127	0.0921	0.0303	0.1298
T_3	0.1114	0.2434	0.1678	0.0226
T_4	0.7819	1.7333	1.2871	1.0356

Table 3
The PSO best values according to the different parameter sets and various control signals.

c_1	c_2	The best values of the PSO algorithm			
		m_1	m_2	δ_1	δ_2
1.3	1.3	0.1804	0.3380	2.1109	2.0092
1.7	1.7	0.1613	0.3321	2.0904	2.0108
2	2	0.1591	0.3160	1.8933	2.0078
1.3	2	0.1668	0.3278	2.0059	2.0129
2	1.3	0.1643	0.3302	2.1880	2.0266

Table 4
The optimization results of the different algorithms.

Control signal	Optimization methodology	Fitness function best value	Fitness function mean value	CPU time (s)
m_1	PSO	0.1591	0.6905	251
	GA	2.0181	2.1106	578
	CEP	0.8004	1.9333	370
m_2	PSO	0.3160	0.7729	387
	GA	0.6077	0.9925	473
	CEP	0.4346	0.8744	453
δ_1	PSO	1.8933	3.6741	345
	GA	2.1220	4.0903	594
	CEP	4.0788	4.5510	483
δ_2	PSO	2.0078	4.1007	313
	GA	4.7223	5.2022	546
	CEP	5.0003	6.1051	489

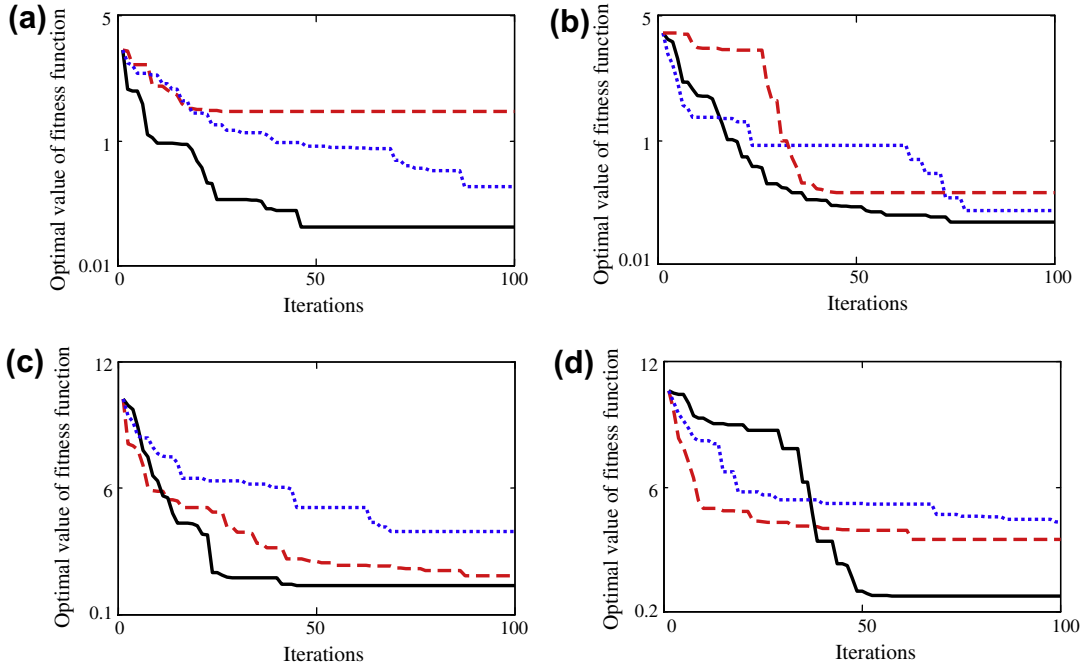

Fig. 8. Convergence curves of the Fitness function for (a) m_1, (b) m_2, (c) δ_1, (d) δ_2: Solid (PSO), Dashed (GA), Dotted (CEP).

In the ITSE, the advantage of the time weighting will be counteracted due to the squaring of the value of the error, because the values of the squared small errors become very close to zero [27] and thus the optimizers may be stuck in the local optima instead of the global solutions.

As it is assumed in Table 1, the operating points are selected in a way in which the generations in both areas experience a wide range of productions and loadability.

The optimization process is enchained to some bounded constraints as:

$$\begin{aligned} &K^{min} \leqslant K \leqslant K^{max} \\ &T_1^{min} \leqslant T_1 \leqslant T_1^{max}, \quad T_2^{min} \leqslant T_2 \leqslant T_2^{max} \\ &T_3^{min} \leqslant T_3 \leqslant T_3^{max}, \quad T_4^{min} \leqslant T_4 \leqslant T_4^{max} \end{aligned} \tag{27}$$

The optimized damping controller parameters using the PSO algorithm and by satisfying the defined objective function and constraints are displayed in Table 2. In the optimization process, each of four control signals is modulated as a lead-lag damping controller and applied separately to the power system. It should be noted that to obtain the optimistic damping performance, number of particles, particle size, number of iterations, c_1 and c_2 are chosen as 50, 5, 100, 2 and 2, respectively. It should be mentioned that with the aim of reducing the risk of stuck in an undesired local optimal point, the optimization procedure via the PSO algorithm is repeated several times to be sure the global optimum is obtained.

In order verify that the PSO parameter sets (i.e. c_1 and c_2) are designated in an appropriate way which fits to the study, different set of the c_1 and c_2 parameters are picked and the best value of the fitness function corresponding to the different control signals are computed. The results listed in Table 3, verify the sufficiency of election the values of $c_1 = 2$ and $c_2 = 2$ to this study. Moreover, in Table 4, the results of the optimization framework are summarized in the terms of the best, the mean values of the objective function and also the CPU time corresponding to all algorithms. The convergence ratios for different control signals and using the PSO, GA and CEP algorithms are also shown in Fig. 8. The results are clearly demonstrated that the PSO algorithm has a superior function in the terms of convergence ratio and obtaining the hithermost solution to the global optima.

CPU time or (process time) is the amount of time for which a central processing unit (CPU) was used for processing instructions of a computer program. Some methods are very capable of reaching the goal whereas they are time consuming inasmuch as they cannot be used in real world applications. All the programs in this study were simulated in the MATLAB R2009b environment with CPU 2.2 GHz, Intel core2 Duo processor T6600. Table 3 compares the algorithms in aspect of their one iteration CPU time (units are in second).

In this study, the set of estimators of medians directly from the average error results is computed. Table 5 shows the estimations computed for each algorithm. Focusing our attention in the rows

Table 5
Contract estimation results.

	PSO	GA	CEP
PSO	0	3.2411	3.6929
GA	3.2411	0	0.4518
CEP	3.6929	0.4518	0

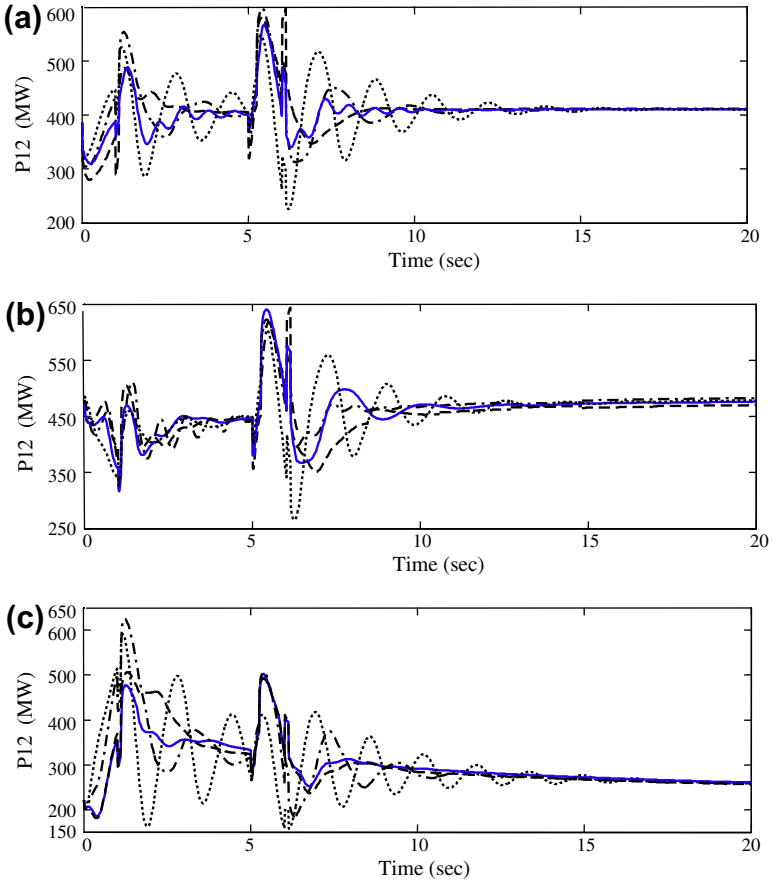

Fig. 9. Tie-line power variations: (a) Case 1, (b) Case 2 and (c) Case 3: Solid (m_1), Dashed (m_2), Dash-Dotted (δ_1) and Dotted (δ_2).

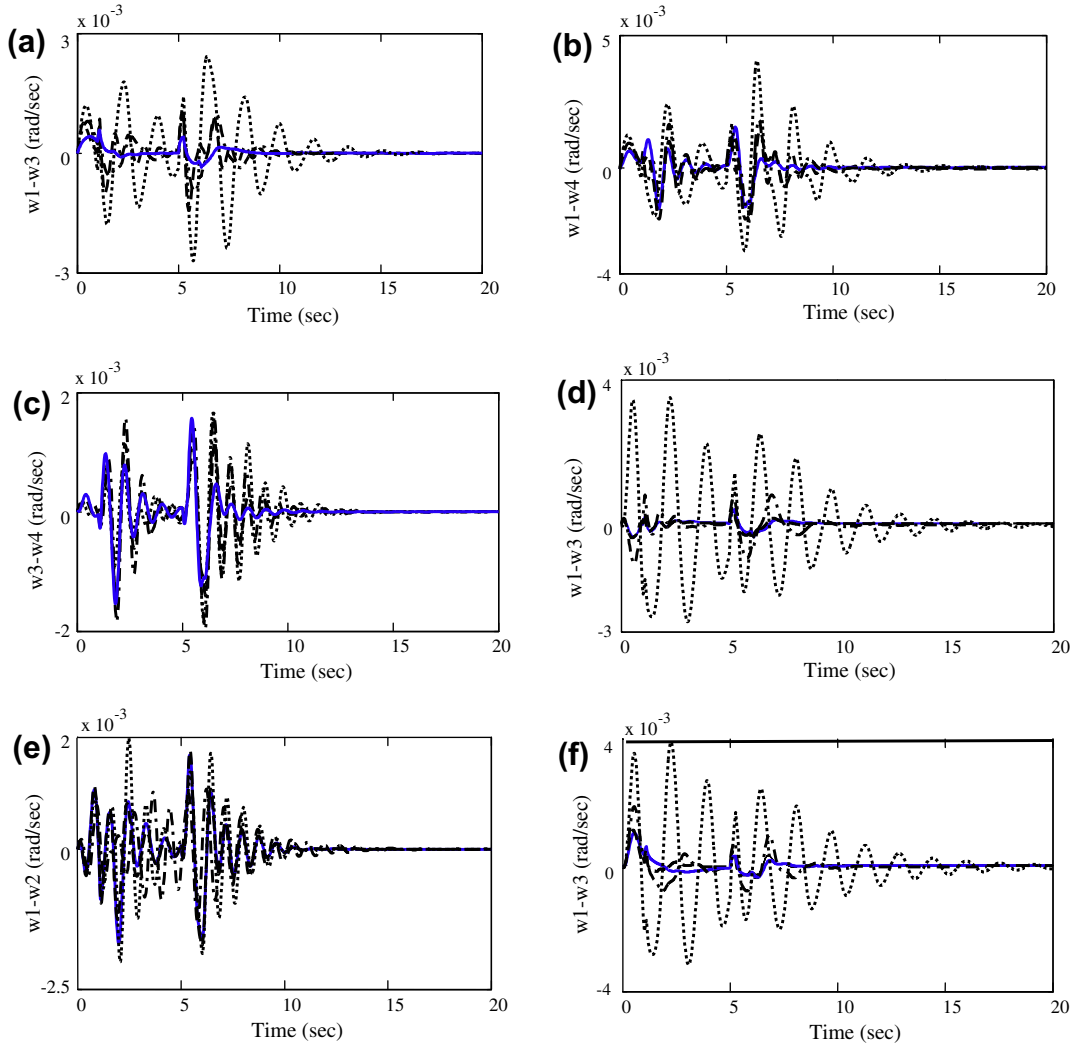

Fig. 10. Speed deviations for some of the inter-area and local modes: (a and b) Case 1, (c and d) Case 2 and (e and f) Case 3: Solid (m_1), Dashed (m_2), Dash-Dotted (δ_1) and Dotted (δ_2).

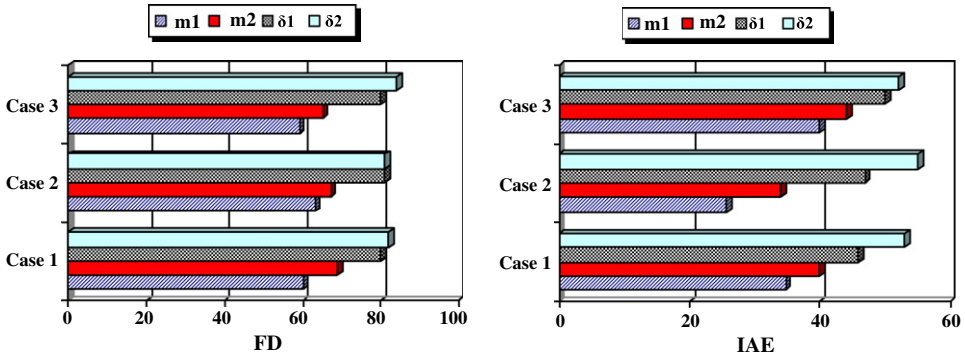

Fig. 11. IAE and FD performance index values using the PSO algorithm.

of the table, we may highlight the performance of PSO (all its related estimators are negative; that is, it achieves very low error rates considering median estimators); on the other hand, CEP and GA achieve higher error rates in this study.

To verify the robustness of the optimum designed damping controllers for the quad control signals of the IPFC, a severe bisection disturbance through two reel 3-phase faults is applied to the power system. In the considered scenario, two sequential three phase faults are occurred in the middle of the line 7–9 in $t = 1$ and $t = 5$ s, respectively. In the later one, the faulted line is tripped permanently but in the first one the fault is cleared without any changes in the system configuration and after 150 msec. The nonlinear time domain simulation results are shown in Figs. 9 and 10. Also, in Fig. 9 the dynamic response of the tie-line power transfer

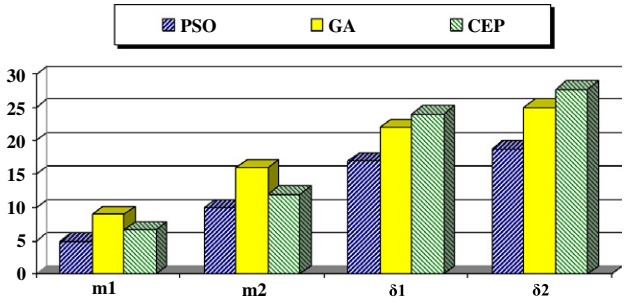

Fig. 12. ITSE performance index values using different algorithms.

signal to the disturbance is represented for all operation cases in Table 1. In Fig. 10 the local and inter-area mode oscillations related to both areas are displayed in some operation cases. Note that the response of all four IPFC control signals (m_1, δ_1, m_2 and δ_2) are shown altogether. Observing Figs. 9 and 10 demonstrates the more efficient damping effect of the m_1 control signal.

Moreover, to demonstrate the effectiveness of the damping controllers' performance two performance indices in terms of the Integral of Absolute value of Error (IAE) and Figure of Demerit (FD) as shown in Fig. 11. Eqs. (28) and (29) are the formation of the performance indices:

$$\mathrm{IAE} = 100\int_0^{t_{sim}} (|\omega_1-\omega_2|+|\omega_1-\omega_3|+|\omega_1-\omega_4|+|\omega_3-\omega_4|)dt \tag{28}$$

$$\mathrm{FD} = (\mathrm{OS}\times 1000)^2 + (\mathrm{US}\times 2000)^2 + T_s^2 \tag{29}$$

where ω_i is the speed of ith generator and OS, US and T_s are indicate overshoot, undershoot and the settling time of the time-domain dynamic response of the '$\omega_1-\omega_3$' signal. So that the FD index significantly describes the damping of the inter-area modes. The smaller value of these indices validates the better performance of damping controller. The values of the IAE and FD indices are confirms that m_1 control signal made the paramount damping controller. The fact which is self explaining from the results is the effectiveness of the proposed current injection model of the IPFC in enhancing the power system stability and all range of the operating points.

For the sake of better demonstration of the performance of the optimization algorithms, the ITSE performance index (Integral of Time multiplied Squared value of the Error) is formulated as in Eq. (30) and applied to the damping controller design problem. The numerical results are depicted in Fig. 12. As shown in Fig. 12, the PSO in the case of the m_1 control signal has the best performance with respect to the other optimization cases.

$$\mathrm{ITSE} = 10{,}000\sum_{k=1}^{Np}\int_0^{t_{sim}} t\cdot(|\omega_{1k}-\omega_{2k}|^2+|\omega_{1k}-\omega_{3k}|^2 + |\omega_{1k}-\omega_{4k}|^2+|\omega_{3k}-\omega_{4k}|^2)dt \tag{30}$$

5. Conclusions

In this paper, in order to enhance the power system stability margins a novel current injection model for the IPFC was carried out. To evaluate the effectiveness of the proposed model a supplementary damping controller under the dynamic equations of a multi-machine power system was designed. The problem of the controller design formulated as an optimization problem under wide range of operating conditions and considering to a severe disturbance. To find out the optimistic set of controller parameters the PSO algorithm was employed. The nonlinear time domain simulation results demonstrate the robustness and advantageous performance of the proposed current injection model and its corresponding designed controller. Moreover, with the objective of identification of the most stabilizer control signal of the IPFC, two performance indices in the terms of the ITSE, IAE and FD were applied to assess the four control signals. Further, by modulating the IPFC all four control signals and through the assessment of the numerical results of applied indices, it was confirmed that the m_1 control signal has superior damping performance comparing to the others. Beside, in order to ensure from the obtaining the optimized solution, the performance of the PSO algorithm is compared to the GA and CEP algorithms. The results validate the superior performance of the PSO algorithm.

References

[1] Machowski J, Bialek JW, Bumby JR. Power system dynamics and stability. Chichester: John Wiley & Sons; 1997.
[2] Ali ES, Abd-Elazim SM. Coordinated design of PSSs and TCSC via bacterial swarm optimization algorithm in a multimachine power system. Int J Electr Power Energy Syst 2012;36:84–92.
[3] Hingorani NG, Gyugyi L. Understanding FACTS: concepts and technology of flexible AC transmission systems. New York: IEEE Press; 2000.
[4] Gyugyi L, Sen KK, Schauder CD. The interline power flow controller concept: a new approach to power flow management in transmission systems. IEEE Trans Power Deliv 1999;14:1115–23.
[5] Mishra S, Dash PK, Hota PK, Tripathy M. Genetically optimized Neuro-Fuzzy IPFC for damping modal oscillations of power system. IEEE Trans Power Syst 2002;17(4):1140–7.
[6] Banaei MR, Kami A. Interline power flow controller (IPFC) based damping recurrent neural network controllers for enhancing stability. Energy Convers Manage 2011;52:2629–36.
[7] Safari A, Rezaei N. Robust design a PSO based IPFC output feedback damping controller. Res J Appl Sci – Eng Technol 2012;4(2):206–13.
[8] Parimi AM, Elamvazuthi I, Saad N. Interline power flow controller (IPFC) based damping controllers for damping low frequency oscillation in power system. ICSET 2008:334–9.
[9] Azbe V, Mihalic R. The control strategy for an IPFC based on the energy function. IEEE Trans Power Syst 2008;23(4):1662–9.
[10] Fuerte-Esquivel CR, Acha E, Ambriz-Perez H. A comprehensive Newton–Raphson UPFC model for the quadratic power flow solution of practical power networks. IEEE Trans Power Syst 2000;15(1):102–9.
[11] Zhihui Y, deHaan SWH, Ferreira B. Utilizing distributed power flow controller (dpfc) for power oscillation damping. Proc IEEE Power Energy Soc Gen Meet (PES) 2009:1–5.
[12] Son KM, Lasseter RH. A Newton-type current injection model of UPFC for studying low-frequency oscillations. IEEE Trans Power Deliv 2004;19(2):694–701.
[13] Shayeghi H, Shayanfar HA, Jalilzadeh S, Safari A. TCSC robust damping controller design based on particle swarm optimization for a multi-machine power system. Energy Convers Manage 2010;51:1873–82.
[14] Vinkovic A, Mihalic R. A current-based model of the static synchronous series compensator (SSSC) for Newton–Raphson power flow. Electr Power Syst Res 2008;78(10):1806–13.
[15] Zhang Y, Zhang Y, Chen C. A novel power injection model of IPFC for power flow analysis inclusive of practical constraints. IEEE Trans Power Syst 2006;21(4):1550–6.
[16] Vinkovic A, Mihalic R. A current-based model of an IPFC for Newton–Raphson power flow. Electr Power Syst Res 2009;79(8):1247–54.
[17] Mahdad B, Srairi K, Bouktir T. Optimal power flow for large-scale power system with shunt FACTS using efficient parallel GA original research article. Int J Electr Power Energy Syst 2010;32(5):507–17.
[18] Vinkovic A, Mihalic R. Universal method for the modeling of the 2nd generation FACTS devices in Newton–Raphson power flow. Int J Electr Power and Energy Syst 2011;33:1631–7.
[19] Lashkar Ara A, Kazemi A, Nabavi Niaki SA. Modelling of Optimal Unified Power Flow Controller (OUPFC) for optimal steady-state performance of power systems. Energy Convers Manage 2011;52:1325–33.
[20] Del Valle Y, Venayagamoorthy GK, Mohagheghi S, Carlos J, Harlry RG. Particle swarm optimization: basic concepts, variants and application in power systems. IEEE Trans Evol Comput 2008;12:171–95.
[21] Chen MR, Li X, Lu YZ. A novel particle swarm optimizer hybridized with external optimization. Appl Soft Comput 2010;10:367–73.
[22] Kennedy J, Eberhart R. Particle swarm optimization. In: Proceedings of IEEE international conference on neural networks; 1995. p. 1942–8.
[23] Rini DP, Shamsuddin SM, Yuhaniz SS. Particle swarm optimization: technique, system and challenges. Int J Comput Appl 2011;14(1):19–27.
[24] Chao Lu, Jennie Si, Xiaorong Xie. Direct heuristic dynamic programming for damping oscillations in a large power system. IEEE Trans Syst Man Cybern – Part B Cybern 2008;38(4):1008–13.
[25] Kundur P. Power system stability and control. New York: Mc-Grall Hill; 1994.

[26] Panda S. Robust coordinated design of multiple and multi-type damping controller using differential evolution algorithm. Int J Electr Power Energy Syst 2011;33:1018–30.
[27] King M, King My. Process control: a practical approach. Willey; 2010.
[28] Holland JH. Adaptation in natural and artificial system. University of Michigan Press; 1975.
[29] Randy A, Haupt L, Haupt BSE. Practical genetic algorithms. John Wiley & Sons; 2004.
[30] Fogel GB, Greenwood GW, Chellapilla K. Evolutionary computation with extinction: experiments and analysis. In: Proceedings of 2000 congress on evolutionary computation, Piscataway, US; 2000.
[31] Derrac J, García S, Molina D, Herrera F. A practical tutorial on the use of on parametric statistical tests as a methodology for comparing evolutionary and swarm intelligence algorithms. Swarm Evol Comput 2011;1:3–18.
[32] Doksum K. Robust procedures for some linear models with one observation per cell. Ann Math Stat 1967;38:878–83.
[33] García S, Fernández A, Luengo J, Herrera F. Advanced nonparametric tests for multiple comparisons in the design of experiments in computational intelligence and data mining: experimental analysis of power. Inform Sci 2010;180:2044–64.